

ELECTROSTATIC DISCHARGE PROPERTIES OF SELECTED
VOYAGER SPACECRAFT MATERIALS*

J. B. Barengoltz
Jet Propulsion Laboratory
California Institute of Technology

R. B. Greigor II, L. B. Fogdall and S. S. Cannaday
Boeing Aerospace Company

ABSTRACT

As a part of an extensive program to assess and ameliorate the electrostatic discharge hazard to the Voyager spacecraft posed by passage through the charged particle environment near Jupiter, a testing activity to characterize the behavior of selected Voyager materials was undertaken. A series of twelve material and component samples were exposed to an electron beam in order to measure the time history and amplitude of resultant electrostatic discharges. These tests were conducted at a Boeing Aerospace Company combined radiation effects test chamber.

The typical experimental design was to mount the test article with its dielectric surface facing the beam and its conductive portion isolated from ground except by way of a shielded cable on which a discharge pulse could be observed. The behavior of the sample was then observed at bombarding energies from 20 to 100 keV in increasing 20 keV increments and then 90 to 30 keV in decreasing 20 keV increments. Observations were made at each energy for nominally two hours at an electron flux of $4 \times 10^9 \text{ cm}^{-2} \text{ s}^{-1}$.

INTRODUCTION

The differential electrical charging of spacecraft surfaces in a charged particle environment is a recognized subject of interest to spacecraft designers. This effect was originally a matter for the scientific instruments such as charged particle spectrometers where the measured spectrum would be offset. However, the observed correlation between anomalous effects in the electronics of geosynchronous satellites and magnetic substorms is a strong indication of differential charging and subsequent electrical discharges (Ref. 1).

The Voyager Project established an extensive program (Ref. 2) to assess and minimize this electrostatic discharge (ESD) hazard for the two Voyager spacecraft which will encounter the radiation environment near Jupiter. This

*This work presents the results of one phase of research carried out at the Jet Propulsion Laboratory, California Institute of Technology, under contract No. NAS7-100, sponsored by the National Aeronautics & Space Administration.

program's objective was to design the spacecraft so as to eliminate the hazard and to demonstrate through testing and analysis that the goal had been met. Components of this program included analyses of the differential charging, due to electrons, protons, and the photoelectric effect, of the Voyager spacecraft (performed by Sanders, et al. of TRW (Ref. 3)), a systematic design process to eliminate wherever possible exposed dielectrics from the spacecraft, simulated ESD tests of the spacecraft, and the computer code Systems Electromagnetic Analysis Program (SEMCAP) (TRW). The work described in this paper was intended to characterize the remaining suspect materials (from an ESD viewpoint) and to provide values for the magnitude of possible discharges. This data was required to ensure that the simulated ESD tests were adequately severe, and as input to SEMCAP, which was used to predict potential adverse subsystem responses and verify that corrective measures were appropriate.

Procedure

A series of twelve material and component samples from the Voyager spacecraft were exposed to an electron beam in order to measure the time history and amplitude of resultant electrostatic discharges. The test articles were FEP teflon, a section of magnetometer boom longeron with a piece of bare cable braid mounted on it, a section of longeron with a piece of jacketed cable mounted on it, a piece of the magnetometer cable (alone), a flight Brewster plate, a piece of plume shield, a section of the high gain antenna, a piece of the frequency selective subreflector, a separation connector, a piece of thermal blanket, a sample of the radioisotopic thermoelectric generator (RTG) case coating, and an end dome of an RTG case (Table 1). In general, these test articles can be categorized as follows: (1) planar dielectric/conductor structures (teflon, Brewster plate, high gain antenna); (2) non-planar dielectric/conductor structures (magnetometer boom longeron, frequency selective subreflector, separation connector); and (3) structures of unknown dielectric tendencies.

The samples were exposed in one of two Boeing combined radiation effects test chambers (CRETC) (Fig. 1). These systems are clean vacuum systems with fluidless pumping and glass, ceramic, and metal seals and with provisions for the simultaneous exposure of a sample to electrons, protons and ultraviolet. In these tests only the electron source was employed, at energies ranging from 20 to 100 keV and a flux of $4 \times 10^9 \text{ cm}^{-2} \text{ s}^{-1}$.

The electron energy was calculated from the known electron gun cathode potential with a loss in the aluminum scattering foil based on range-energy tables. A rotatable Faraday cup was employed to measure the electron beam profile after the spreading by the foil. A second, fixed Faraday cup was standardized for the flux at sample center and then used to monitor the electron beam during the exposure of a sample.

The test articles were mounted so that the dielectric surface, i.e., the exposed surface in spacecraft use, was facing the electron beam (Fig. 2, 3, & 4). The conductive part of the test article was isolated from ground except by way of a shielded cable on which a discharge pulse could be observed. This signal cable was connected to ground through a 50 Ω resistor for impedance

matching. The discharge pulses were measured by a fast rise-time current probe on the ground wire or the voltage across the resistor. The measured pulses were displayed on a wide bandwidth 7000 series Tektronix scope with fast writing speed (2cm ns^{-1}) and recorded by a Polaroid camera. A simple loop antenna was also located in the chamber to count all events, including those too small to trigger the pulse measurement circuit.

The general test procedure was to expose the sample to electrons at energies from 20 to 100 keV in 20 keV increments and then 90 to 30 keV in 20 keV decrements. At each energy observations were made for about two hours.

Test Results

A summary of the test results is provided in Table 2. Without exception, all of the samples known to be dielectric/conductor structures exhibited single pulse discharge-like events (See, e.g. Fig. 5). These samples are the teflon, magnetometer boom longeron (with cable or cable braid), Brewster plate, high gain antenna, frequency selective subreflector and the separation connector. Conversely all of the samples whose exposed dielectric surfaces had been modified during the Voyager ESD program to enhance conductivity and confer ESD immunity exhibited only atypical events. The signal from an atypical event was similar to a damped oscillation with a fast frequency (0.25 to 0.50 ns^{-1}) and a decay period of 50 to 200 ns. These samples were the magnetometer cable (alone) and the thermal blanket. The teflon outer insulation of the cable had been replaced by a wrap of "conductive" teflon tape. Similarly the outer Kapton surface of the thermal blanket had been painted with a "conductive" Sheldahl paint.

Of the doubtful dielectrics, the plume shield produced three single-pulse signals during its entire exposure and a larger number of atypical events. The sample exposed had a black, low-conductivity surface as supplied (perhaps an oxide layer). The two different sized samples of RTG case were observed to yield only atypical signals, however (Fig. 6, 7 & 8). There is some uncertainty about the resistivity of the iron titanate (in a borosilicate matrix) coating involved, but it is much less than all materials except the "conductive" teflon and Sheldahl.

DISCUSSION

The teflon results lend themselves to analysis because of the planar geometry and the known breakdown voltage of the material. In addition, the special sample holder employed (Fig. 2) drastically reduced edge effects by beam masking. Thus one expects a total surface charge of $11.6\mu\text{C}$ from the calculated capacitance and a breakdown voltage of 17.5 kV. The charge observed in the largest single discharge (determined by integration of the current pulse) was in fact $12\mu\text{C}$ (Fig. 5).

This result contrasts to some extent with the findings of Stevens, et al. (Ref. 4) of a "replacement" charge of $15\mu\text{C}$ (measured as in this work) for a measured discharge of 50 to $60\mu\text{C}$ in $127\mu\text{m}$ (5 mil) FEP teflon. Stevens, et al. determined the actual discharge from the surface potential before and after

breakdown and a measurement of the sample effective capacitance by the surface charge and voltage dependency during charging. They concluded that the "replacement" charge does not appear to compensate for all of the charge lost in the discharge. As noted in their work, however, edge effects are very important. The expected surface charge for their larger sample would be 66 μ C on the basis of the ideal capacitance and breakdown voltage (compared to 11.6 μ C for this work). However, the edge effects lowered the observed breakdown voltage to 12 kV from 17.5 kV and evidently increased the effective capacitance from 3.8 nF to a value between 4.2 and 5.0 nF. Since edge effects drastically lowered the breakdown potential, perhaps much of the missing charge was an edge breakdown.

A comparison of the maximum currents observed in this work and Reference 4 shows them to be approximately commensurate (250A vs. 100A, respectively). Even if a factor of 3 to 4 is applied to the previous work's result to predict an arc discharge of 300 to 400A, this conclusion is unchanged. Further, the pulse widths observed have a ratio of about 10 and the discharge charges about 5 (in the opposite sense). It appears that in the absence of edge effects, the total charge is observed and scales with area (a factor of 6). However, the pulse width also scales with the area (an RC constant), so that the peak current is not dependent on surface area. Edge discharging evidently causes part of the current not to be observed as "replacement" current and lengthens the duration of the "replacement" signal.

The magnetometer boom longeron section and cable braid test (Fig. 3) produced a very interesting result. During the exposure of this sample the charging of the fiberglass longeron caused a force which attracted the flexible cable braid. The braid was observed to bow out, contact the relatively stiff longeron, and occasionally remain in contact for periods up to fifteen minutes. The subsequent sudden release was always correlated with the observation of a discharge signal. After the test a direct measurement of the force required to produce this observation set the value at 0.11 N. A calculation of the force in terms of a uniform line of charge parallel to a cylindrical conductor leads to a total charge on the longeron of 8.8×10^{-8} C. In terms of capacitance and breakdown voltage, the 15-cm section corresponded to 8.6pF charged to -10.2kV. The maximum observed charge was 4×10^{-8} C on a 5A discharge event. The simplest explanation of the observation of only part of the possible total arc charge is that the discharge was partial due to the braid springing back and the limited region of original contact. In any event at least one half of the arc charge was observed in the "replacement" signal. Edge effects were also operative since the cable braid was mounted on the longeron by conductive "knuckles". Therefore any discharge from this spacecraft component is limited to that from a section between adjacent "knuckles".

The atypical pulses are the most difficult result to understand. On the basis of their appearance in the low resistivity samples only, the hypothesis of a burst of very small local discharges is attractive. The damping would then be due to mutual inductance of these several parallel breakdown paths. The resistively damped LRC oscillation interpretation is supported by the observed change in the appearance of the signals from the RTG case end dome when an external 47 μ H inductor was placed in parallel to the external

resistor (Figs. 7 and 8). The plume shield may have been an intermediate case with its thin oxide layer, i.e., some global discharges and some local discharges.

This picture is enhanced by an extra test conducted on a stainless steel sample of the size of the RTG case coating sample. During the first three hours, this dummy sample exhibited three atypical pulses similar to the RTG case coating results. Then no more events were observed. Apparently, there were some localized areas of surface contamination which cleaned up due to the vacuum and the electron beam.

CONCLUSIONS

Twelve material and component samples of the Voyager spacecraft have been evaluated in terms of their electrostatic discharge tendencies. As expected all of the test articles exhibited some discharge phenomena when exposed to an electron beam. An important unexpected result was the appearance of a damped oscillating discharge from the poor insulators in contrast to a simple pulse signal from the good insulators.

Of direct interest to the spacecraft ESD question is the demonstrated possibility of a global or complete discharge from a dielectric. The current pulse as measured represents a charge commensurate with the actual discharge (a factor of 0.5, say) provided that edge effects are absent or minimized. This can be accomplished by masking the edges of the sample from the beam. The peak current probably does not scale with surface area. Insulator thickness will affect the value through the breakdown voltage, however. The arc charge probably scales with capacitance, while the pulse width is likewise proportional to capacitance. The atypical discharges from the poor insulators appear to be a series of local discharges. As such, none of the parameters would scale with sample surface area.

Further systematic research would be desirable to place some of these tentative conclusions on a firmer basis, especially the "replacement" current/arc current and the scaling hypotheses. For analysis of circuit susceptibility to discharges in nearby insulators, an arc rise time model is required. Finally, the sense of the observed current, electrons flowing into the conductor from the external circuit, is difficult to explain with any simple discharge model. A good model would be indispensable in conjunction with research yet to be accomplished.

REFERENCES

1. Rosen, A. "Spacecraft Charging: Environment-Induced Anomalies", Journ. of Spacecraft and Rockets 13, No. 3 (1976).

2. Whittlesey, A.C., "Voyager Electrostatic Discharge Protection Program", 1978 IEEE International Symposium on Electromagnetic Compatibility, June 20-22, 1978, IEEE CH1304 (1978).
3. Sanders, N. L., Inouye, G.T., and Rosen, A., "Voyager Spacecraft Charging Immunization Support to JPL; TRW No. 31440-6002-RU-00, (1977).
4. Stevens, N. J., Berkopec, F.D., Staskus, J.V., Blech, R.A., and Narisco, S. J., "Testing of Typical Spacecraft Materials in a Simulated Substorm Environment", NASA TM X-73603 (1976) (also published in proceedings of the Conference on Spacecraft Charging Technology, October 27-29, 1976, NASA TM X-73537).

TABLE 1. - PHYSICAL PROPERTIES OF SAMPLES TESTED

TEST ARTICLE	DIELECTRIC SURFACE			CAPACITANCE (pF)
	COMPOSITION	THICKNESS (μm)	AREA (cm^2)	
FEP TEFLON	FEP TEFLON	127	50	630
LONGERON/CABLE BRAID	FIBERGLASS	N/A	N/A	8.6
LONGERON/MAG CABLE	FIBERGLASS/TEFLON*	N/A	N/A	?
MAG CABLE	TEFLON*	63	45.6	?
BREWSTER PLATE	EPOXY	50	620	38,000
PLUME SHIELD	NICKEL OXIDE	?	50	?
HIGH GAIN ANTENNA	PV-100 PAINT	100 (NOM)	290	2500
FREQUENCY SELECTIVE SUBREFLECTOR	PV-100 PAINT	100 (NOM)	N/A	14 (EST)
SEPARATION CONNECTOR	PHENOLIC	N/A	N/A	150 (EST)
THERMAL BLANKET	SHELD AHL*	25 (NOM)	50	?
RTG CASE PIECE (END DOME)	IRON TITANATE BOROSILICATE MATRIX	50-75	25 (700)	3 (10,000)

* INTENDED TO BE CONDUCTIVE

TABLE 2. - SPACECRAFT MATERIALS DISCHARGE TEST RESULTS SUMMARY

TEST ARTICLE	TYPICAL MEASURED PULSE ^a		
	RISE TIME (ns)	WIDTH (ns)	AMPLITUDE (A)
FEP TEFLON	30	50-300	20-250
LONGERON/CABLE BRAID	2	5	0.5-6
LONGERON/MAG CABLE	4-10 N/A	10-20 N/A	0.8-2 (BRAID) (0.08-0.8) ^b (WIRE)
MAG CABLE	N/A N/A	N/A N/A	0.5-5 ^b (BRAID) (1V) ^b (WIRE)
BREWSTER PLATE	1.5-10	4-20	0.1-3
PLUME SHIELD	10-40	50-300	0.05-0.3
HIGH GAIN ANTENNA	2-10	8-20	0.1-0.4
FREQ SELECTIVE SUBREFLECTOR	2-8	8-80	0.1-8
SEPARATION CONNECTOR	10-20	15-30	0.2-18
THERMAL BLANKET	N/A	N/A	2-3 ^b
RTG CASE PIECE	N/A	N/A	0.15-100 ^b
RTG CASE END DOME	N/A	N/A	0.2-5.5 ^b

^aPULSE PARAMETERS, ESPECIALLY AMPLITUDE ARE ENERGY DEPENDENT

^bATYPICAL OSCILLATORY SIGNALS, NO PULSE-LIKE SIGNALS

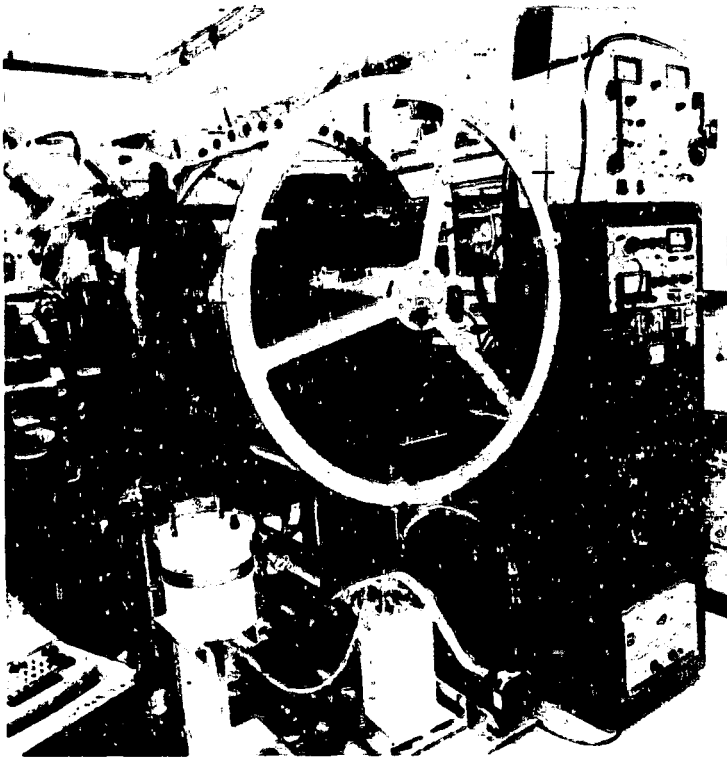


Figure 1. - Combined radiation effects test chamber (CRETC) system.

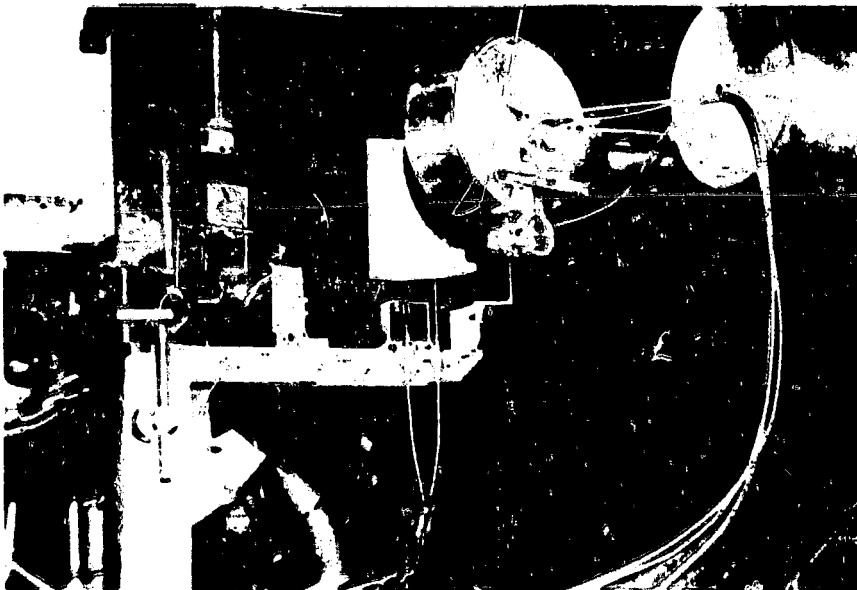


Figure 2. - Teflon test setup.

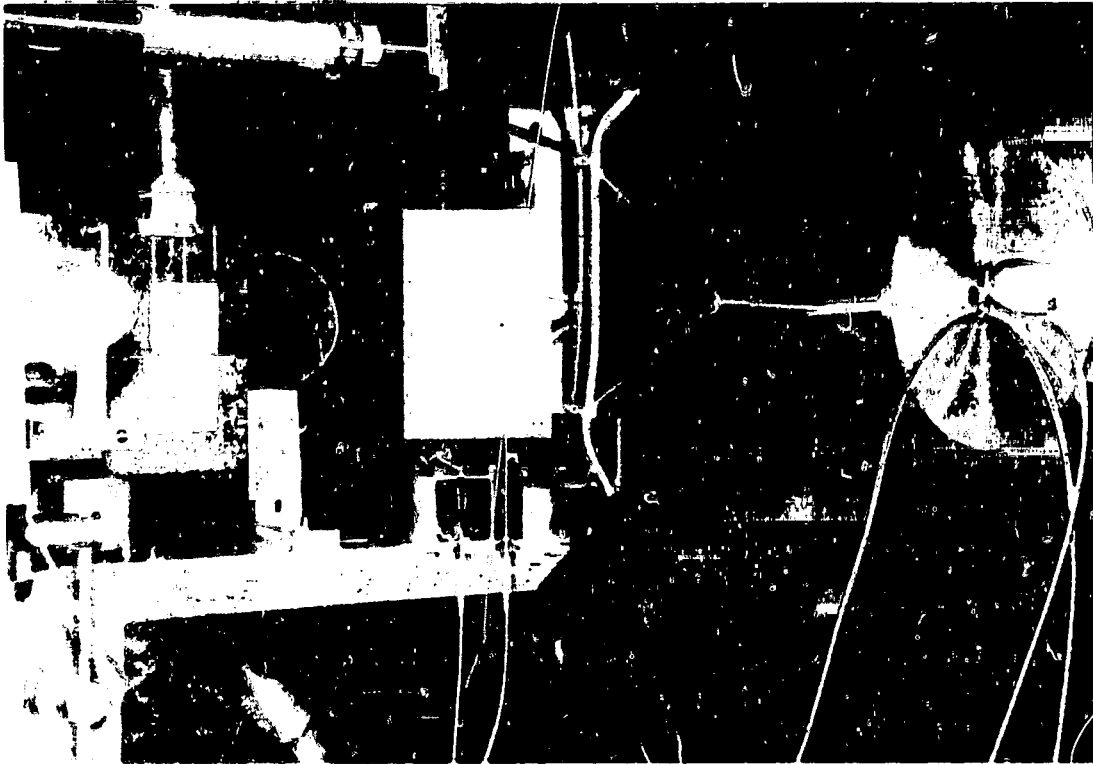


Figure 3. - Longeron and braic test setup.

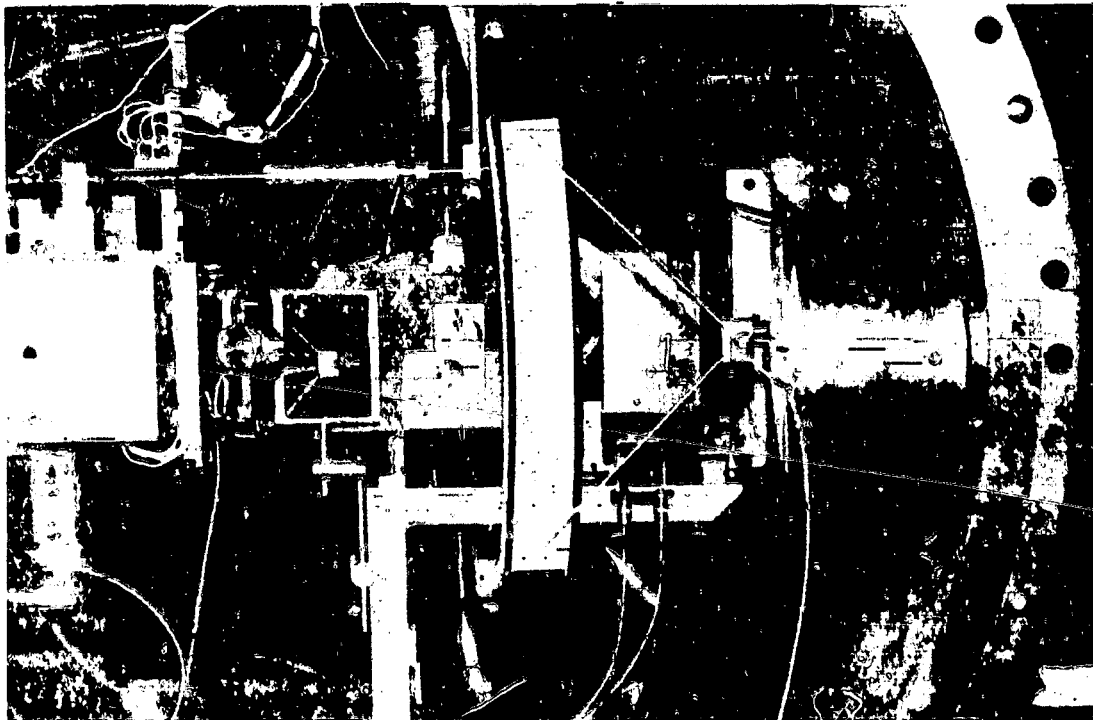


Figure 4. - Antenna section test setup.

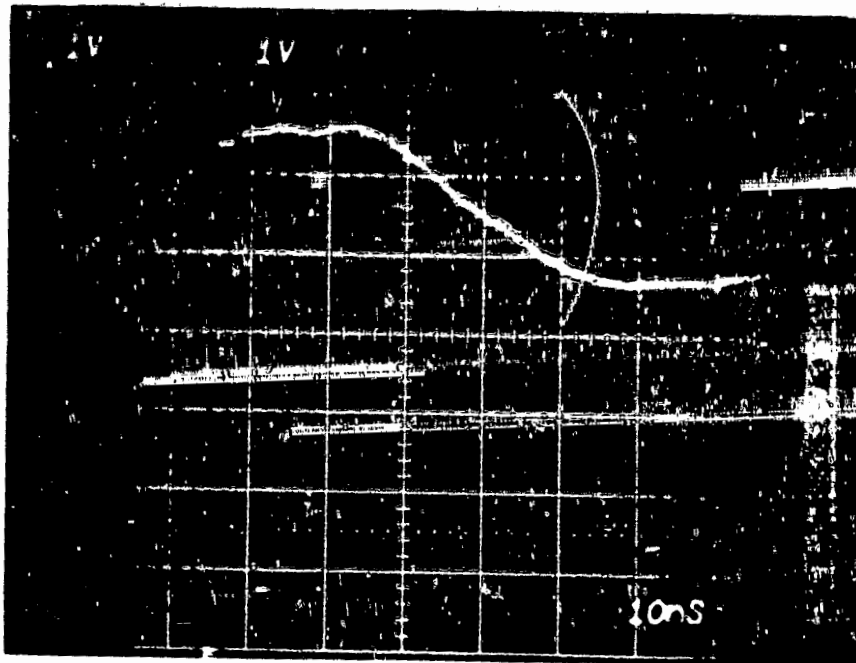


Figure 5. - Teflon loop antenna discharge pulse. Energy, 40 keV; 1 V/division; 100 A/division.

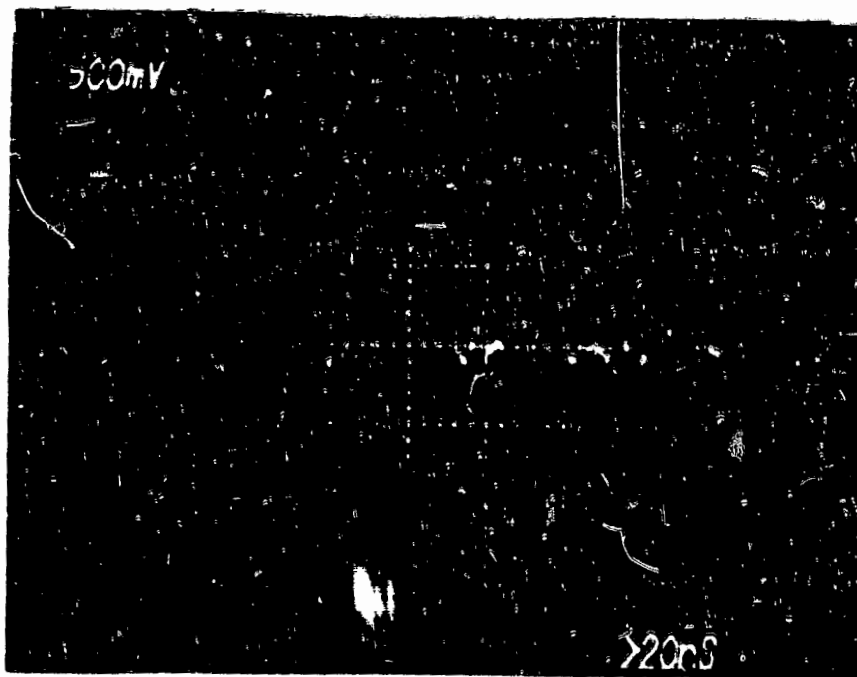


Figure 6. - RTG case strip pulse. Energy, 20 keV; 500 mV/division; 0.2 A/division.

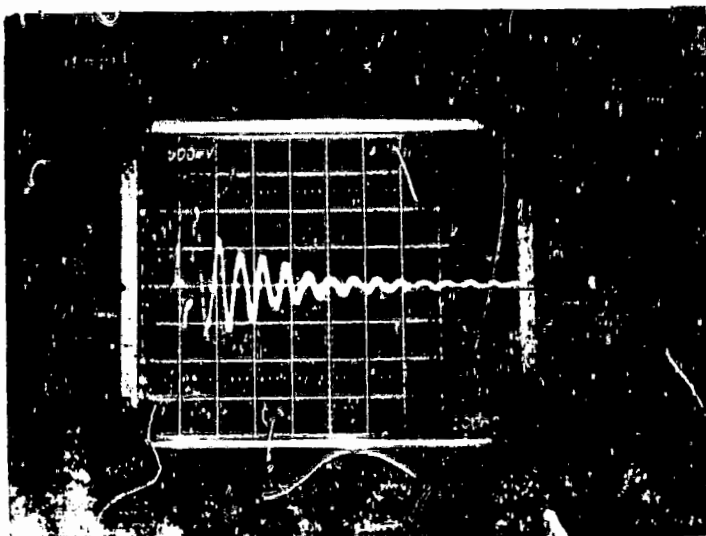


Figure 7. - RTG end dome pulse. Energy, 100 keV (room temperature); 500 mV/division; 1 A/division.

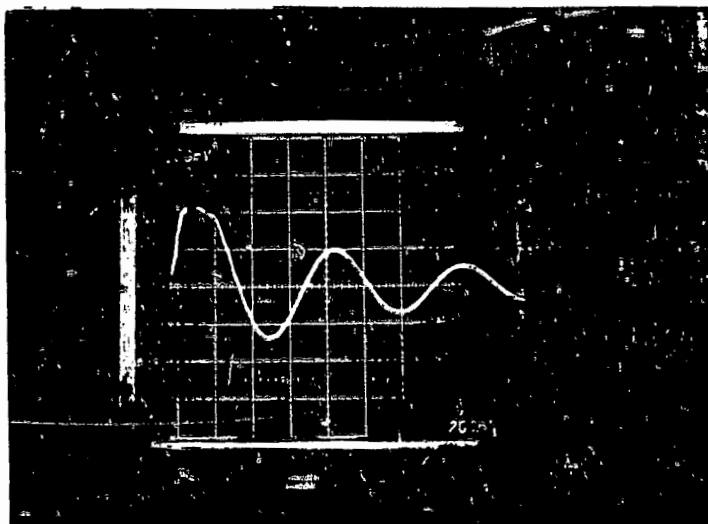


Figure 8. - RTG end dome pulse with 47- μ H external inductor. Energy, 100 keV (room temperature), $L = 47 \mu\text{H}$; 100 mV/division; 0.04 A/division.